Energy Conversion and Management 253 (2022) 115168

Contents lists available at ScienceDirect

Energy Conversion and Management

journal homepage: www.elsevier.com/locate/enconman

Hybrid storage solution steam-accumulator combined to concrete-block to save energy during startups of combined cycles

P.A. González-Gómez *, M. Laporte-Azcué, M. Fernández-Torrijos, D. Santana

Energy Systems Engineering Group (ISE), Department of Thermal and Fluid Engineering, University Carlos III of Madrid, Av. Universidad 30, 28911, Spain

ARTICLE INFO

Keywords:
Combined cycles
Thermal energy storage
Fast startup
Efficiency improvement
Dynamic simulation

ABSTRACT

This work presents a novel steam accumulator and concrete-block storage system (SACSS) to recover part of the energy lost through the steam cycle side during startups of combined cycle power plants (CCPPs). The steam accumulators are integrated with sensible-heat concrete storage to provide superheated steam resulting then to a higher efficiency and safer steam turbine operation compared with systems based only on saturated steam. An economic analysis is performed considering two different scenarios: i) a CCPP able to execute fast startups using a Benson-type heat recovery steam generator (HRSG) and ii) a CCPP operated with conventional startups which employs a typical drum-type HRSG. It is worth mentioning that the second scenario is based on measured data. The economic optimization of the SACSS is carried out focusing in four design variables: number of steam accumulator units, storage pressure, concrete-block length and outer concrete diameter. The optimum solution presents a net present value of 4.45 M€ and a payback period of 3 years for the CCPP suitable for fast startups. For the CCPP operated with conventional startups, a net present value of 2.53 M€ and a payback period of 3.4 years are obtained. The net present value grows around 60 % in both cases if the benefits from carbon credits are considered. In addition to the efficiency improvement, the SACSS could be used to preheat critical sections of the heat recovery steam generators, reducing the thermal stress and the fatigue damage during fast startups. Finally, the emissions avoided thanks to SACSS are estimated to be around 3 640 and 2 175 tons of CO_2 per year, for fast and conventional startup cases, respectively.

1. Introduction

Renewable energies have recently reached a high maturity level and hence they constitute one of the main chances to face global warming by providing clean energy sources, which becomes critical due to the increase of electric energy consumption worldwide. However, its integration into the electric grid system brings a hard challenge since they undoubtedly provide instability issues to the system. In this context, fossil-fueled load-following plants like combined cycles or coal-fired power plants have a key role to meet users demand and to counterbalance grid instability issues related to variable renewable energy sources (VRES) like wind or photovoltaics (PV) [1]. This is somehow the way to compete with higher generation costs compared to VRES, where load-following plants benefit from additional revenues due to the electric grid balance services as spinning reserves, power system stabilization, frequency support, black-start services, etc [2].

In the near future, the problem is likely to be aggravated since the penetration of VRES is expected to grow due to its extremely low generation cost. In the case of Spain (or UE), the penetration of VRES is expect to achieve levels of 75 % by 2030 [3]. In addition, the politics to achieve the decarbonization of the electric system by means of CO_2 taxes will push coal-fired plants to shut down soon. Contrarily, this fact is expected to increase the natural gas consumption in the following years due to its critical role in providing grid stability [3]. Moreover, as it was claimed by Tapetado and Usaola [4], the role of conventional plants will be critical to provide suitable levels of reliability in the electric grid system in the coming years.

In this context, the high penetration of VRES will result in an increase in the number of startups and load changes per year of CCPPs. Furthermore, during the late afternoon periods, load-following plants are expected to provide pronounced ramp-up rates to counterbalance both the down-ramp rates in the PV system and the high demand at such hours. These ramps would be possible if the CCPPs are somehow ready after preheating. In the end, the cycling operating conditions lead to two main problems: i) the annual energy efficiency reduction as a result of both the release of useful energy to ambient due to steam turbine or heat recovery steam generator (HRSG) constraints during startup operation

* Corresponding author.
E-mail address: pegonzal@ing.uc3m.es (P.A. González-Gómez).

https://doi.org/10.1016/j.enconman.2021.115168
Received 29 September 2021; Received in revised form 20 December 2021; Accepted 21 December 2021
Available online 29 December 2021

Nomenclature

Abbreviations

ASME	*American society of mechanical engineers*
CAES	*Compressed air energy storage*
CCPP	*Combined cycle power plant*
ECO	*Economizer*
EV	*Evaporator*
HPT	*High-pressure turbine*
HRSG	*Heat recovery steam generator*
IPT	*Intermediate-pressure turbine*
LAES	*Liquid air energy storage*
K_{st}	*Stodola coefficient* ($K^{0.5}$s m)
k	*thermal conductivity* (W/m K)
L_c	*concrete-block length* (m)
M	*mass* (kg)
$\dot{m}$	*mass flow rate* (kg/s)
N_t	*number of tubes*
N_y	*number of years* (years)
P_c	*carbon credits price* (€/ton)
p	*pressure* (bar)
q	*heat flux* (W/m^2)
r	*radius* (m)
S	*maximum allowable stress* (MPa)
T	*temperature* (°C)
t	*time* (s), *thickness* (m)
V	*volume* (m^3)
v	*velocity* (m/s)
W_t	*steam turbine power* (MW)
z	*cartesian axis direction* (m)
θ	*inflation rate*
ρ	*density* (kg/m^3)
o	*outer*
s	*steam*
t	*tube, turbine*
V	*vessel*
w	*wall*
0	*initial, reference*
LPT	*Low-pressure turbine*
MAPE	*mean absolute percentage error*
MECL	*minimum emissions-compliant load*
NPV	*Net present value*
PCM	*Phase change material*
PV	*Photovoltaics*
RH	*Reheater*
SACSS	*Steam accumulator and*
SH	*Superheater*
VRES	*Variable renewable energy source*

Symbols

A	*cross-sectional area* (m^2)
B_c	*carbon credits benefits* (€)
C_{LP}	*added costs* (USD)
C_T	*total costs* (USD)
C_V	*vessel costs* (USD)
c_p	*specific heat capacity* (J/kg K)
d	*diameter* (m)
E	*joint efficiency factor*
E_{gen}	*generated energy* (MWh)
E_{max}	*energy of low-pressure steam* (MWh)
F_M	*material factor* (-)
F_n	*cash flow* (€)
f	*emission factor* (kgCO2/kWh)
H	*total enthalpy of the fluid* (J)
h	*convective coefficient* (W/m^2K), *specific enthalpy* (J/kg)
I_0	*investment costs* (€)
i	*interest rate* (%)

Greek symbols

α	*thermal diffusivity* (m^2/s)
η_{rec}	*energy recovery efficiency*
η_t	*isentropic turbine efficiency*

Subscripts

c	*concrete*
dis	*discharge*
f	*fluid*
i	*inner*
ins	*insulation*
l	*liquid*

[5], and the increase in the number of hours working at non-optimal conditions due to variable operation, ii) the increase in the amount of thermal cycles and the fatigue damage which will accelerate the failures in the equipment.

The increasing penetration of VRES has changed the operation patterns of CCPPs, since they were designed to operate at based load conditions when the gas prices were low [6]. This new cycling operating conditions have caused an increase in the cycling cost and the forced outages [7]. To solve these issues, a storage system could be employed, which leads to some additional benefits [8]: i) more flexible power plant operation, ii) reduction of the minimum plant load level during storage charging process, iii) increase in the annual energy efficiency of the plant (e.g. recovering energy during fast startups), iv) less frequent plant shutdowns and faster ramping, v) reduction of thermal stresses and increase in the lifetime of plant equipment.

The reduction of the startup times in CCPPs leads to important benefits such as [9]: i) Up to 15 % less fuel consumption. ii) Decrease of the emissions during the startup. iii) Improve the dispatch ranking. This last aspect is very important because the decrease of the startup times directly results in more operating hours for power plants as was shown in [10], mainly due its higher dispatchability. This increases the profitability of the plant if the cycling costs are kept under suitable levels. Due to a demand for fast starts of power plants, original equipment manufacturers offer HRSG specifically designed for that purpose as Benson-type HRSG [11]. It should be highlighted that to this day more than 100 Benson-type HRSGs have been commissioned or are currently being built [12].

Nevertheless, an acceleration of the gas turbine startup could lead to a significant loss of efficiency due to the high amount of energy released to the ambient. In fact, CCPP plants able to execute fast startups requires full (100 %) steam bypass systems to the condenser [11]. Fast gas turbines startups can be made in 20 min independently of the standstill period [13]. However, due to the ramp up constraints of the steam turbine, the complete startup of the CCPP takes around 30–180 min depending on the standstill period [11]. Bearing in mind that this time is computed from the gas turbine ignition to the steam turbine bypass is closed [14] and the maximum steam mass flow for the steam turbine preheating is limited to around the 5 % of the nominal value [14], a high amount of energy is lost through the condenser of the steam cycle in each startup phase. In addition, during fast load-change operations (e.g. responses in the range of 5 min for provision of secondary control reserve), the steam turbine bypass must be also used [15], releasing again potentially useful heat to the condenser. It is worth mentioning that the loss of energy through the steam turbine bypass also occurs in

relatively old CCPPs unsuitable for fast startups [14]. Specially for vintage F class gas turbines which have a minimum emissions-compliant load (MECL) relatively high [11].

Other actuation to accelerate gas turbine startup consist of limiting the inlet mass flow of flue gas into the HRSG by means of a bypass damper [16]. However, flue gas bypass has technical difficulties related to the perfect sealing to prevent leakage of flue gas through the gap between the duct and the damper [11]. Thus, the expected damper leakage leads to a loss of efficiency [17]. As a result, a widely used solution in utility-scale CCPP consist of the installation of high-capacity steam turbine bypass system and dumping the excess of steam into the condenser during a fast startup [11]. This system can also be adapted to CCPPs that were not initially designed for fast startups by retrofitting additional desuperheaters [18]. In fact, due to this more and more frequent practice, a recent survey about HRSG reliability has identified a new additional cause of failure due to the excessive erosion of the steam turbine bypass valves caused by fast startups [19].

In the literature, several projects focused in different energy storage technologies for CCPPs can be found: liquid air energy storage (LAES) [20], compressed air energy storage (CAES) [21], phase change materials (PCMs) [22], thermochemical storage [23], hot water accumulator for district heating [24] and even CCPP hybridized with concentrating solar technology using thermal energy storage [25]. For example, Briola et al. [20] conducted an exergo-economic analysis of a LAES integrated in an existing CCPP as a function of the pressures of the liquid air storage and discharging circuit, for three different economic scenarios (expected, pessimistic and optimistic). They concluded that LAES is profitable in all scenarios except for the pessimistic one, although the high initial costs will result in a large period of amortization. Among the main advantages of LAES it should be underlined its lower thermal inertia and its negligible dependence on the stored mass [26]. Poblete et al. [21] proposed to implement bioenergy storage by means of CAES in a biogas-combined-cycle plant with carbon capture to drive pre-heated turboexpanders during deficit periods. A thermo-economic analysis was carried out for both the biogas-combined-cycle plant with and without carbon capture and CAES, and the results showed a NPV of 2.6 M$ and a payback period of 15 years for the combined-cycle plant without carbon capture and CAES, whereas the NPV and the payback period for the plant with CAES and carbon capture were 0.18 M$ and 33 years, respectively. Li et al. [22] studied the dynamic behavior of a cascade latent heat storage integrated in a 420 MWe CCPP, and they concluded that the proposed system is able to save around 327 GJ (90.83 MWh) of heat from the flue gases bypassed during the start-up operation. However, the proposed system is not able to recover the heat lost through the steam cycle (steam turbine by-pass to the condenser) during the startup phase. In addition, neither the efficiency of the heat recovery during the startup nor the economic viability of the proposed storage system were evaluated. Rao et al. [27] proposed a novel system to store and use the excess energy from intermittent renewable energy sources (e.g. wind power) to preheat the gas in CCPPs in order to reduce the fuel consumption. A PCM-based storage system was proposed in this work, and financial benefits originated from the reduction in fuel consumption were obtained in terms of fuel costs and, to a lesser extent, CO_2 allowance costs for different scenarios. For the optimistic case, a payback period of 8 years was obtained. Although, PCMs-based storage systems have not yet achieved the commercial phase in power generation systems [28], it is a very promising technology to increase the volumetric storage capacity [29]. This technology could be even improved using nano-encapsulated PCM dispersed in fluids [30]. Most of the previous works present an important common drawback: high initial cost and large associated period of amortization. However, the metallic heat capacitor proposed by Angerer et al. [16] ameliorates this issue. This system consists of a thermal buffer storage whose design is based on a matrix of metal plates, placed in the flue gas channel between the gas turbine and the HRSG, which is heated up during startup and cooled down during shutdown, thus reducing the thermal gradients in the HRSG. Their results showed a significant improvement on the lifetime of the high-pressure header of the superheater under fast gas turbine startups. On the other hand, the buffer storage presents two main drawbacks: i) the proposed system does not solve the problem about the high energy lost through the steam cycle (steam turbine by-pass to the condenser) during the startup phase, ii) the increase of the pressure loss in the flue gas flow path induces efficiency penalties at normal operation conditions (e.g. a pressure loss of 2.5 mbar in flue gas flow path leads to a reduction of the whole plant efficiency of 0.15 % [16]), iii) the stored energy can not be managed flexibly. It is worth mentioning that, excluding studies about CCPP hybridized with concentrating solar technology, there is only one work about conventional CCPPs integrating sensible storage system [16].

Out of CCPPs, different works using steam accumulators to enhance the flexibility coal-fired power plants can be found in the literature. For example, Stevanovic et al. [31] propose the use of the stored steam in the steam accumulators to replace the turbine extractions to the condensate heating in low pressure heaters, increasing then the turbine power output under peak demand periods. Richter et al. [32] used the same idea but condensing the steam in the high pressure heaters. Trojan et al. [33] analyzed the use of hot water storage tanks to supply the boiler hot feed water to while the low pressure turbine extraction are suspended to increase the turbine power. An economic analysis was carried out demonstrating the economic profitability of installation of pressure water accumulators.

Based on the literature review, three main conclusions have been obtained:

i. There is a lack of studies dealing with the recovery of the energy lost through the steam cycle side during the startup of CCPPs. This aspect is especially interesting for CCPPs able to execute fast startups because up to the 100 % of the generated steam is bypassed to the condenser during the startup phase [11] and therefore it affects negatively to the plant efficiency.
ii. The economic viability of installing a storage system to recover the energy lost during the startup of CCPPs has not been evaluated yet in the literature. Incorporating the economic analysis for technology-based research is very important to make a decision on the profitability of the proposed system. Furthermore, it is a key aspect to compare objectively different systems.
iii. There is a lack of studies integrating steam accumulators and sensible heat storage to enhance the efficiency of CCPPs, despite these technologies have proven a high maturity state [28].

Concerning about the gap of knowledge shown before, a novel steam accumulator and concrete storage system (SACSS) is presented. The proposed system is specifically designed to recover the energy typically released through the steam cycle (condenser) during the startup phase due to the differences between the gas and steam turbine ramp during the startups. An economic analysis is carried out considering two different scenarios, a CCPP adapted to fast startups using a Benson-type HRSG and a CCPP operated with conventional startups which employs a typical drum-type HRSG. It is worth mentioning that the second scenario is based on measured data. The selection of high-alumina concrete is substantiated on its competitive costs in contrast with other high-temperature sensible storage systems such as magnesia, molten salt, alumina, etc [34]. The high-alumina concrete-block enhances steam outer conditions until reaching superheated state and hence higher efficiencies can be achieved during the discharge. Moreover, SACSS offers additional benefits such as: i) possibility of HRSG preheating to accelerate the gas turbine startup without compromising the lifetime of HRSG components, ii) low installation costs, iii) the stored energy can be delivered flexibly, iv) no additional efficiency penalty is added to the plant when it is operated at normal conditions.

The main objective of this work consists of designing and optimizing economically the SACSS for a CCPP with a regular cycling service

Table 1
Technical data for the CCPP adapted to fast startups using a Benson-type HRSG [5].

Benson HRSG	Steam conditions at turbine and condenser inlet				Steam turbine power	Flue gas conditions in/out
	HP	**RH/IP**	**LP**	**Condenser**		
	p = 128.8 bar	p = 30.8 bar	p = 4.4 bar	p = 0.056 bar	147 MW	$\dot{m}$ = 688.8 kg/s
	T = 565.5 °C	T = 565.1 °C	T = 234.8 °C	T = 35 °C		T_{inlet} = 589.1 °C
	$\dot{m}$ = 77.1 kg/s	$\dot{m}$ = 89.5 kg/s	$\dot{m}$ = 11.3 kg/s			T_{outlet} = 87.7 °C

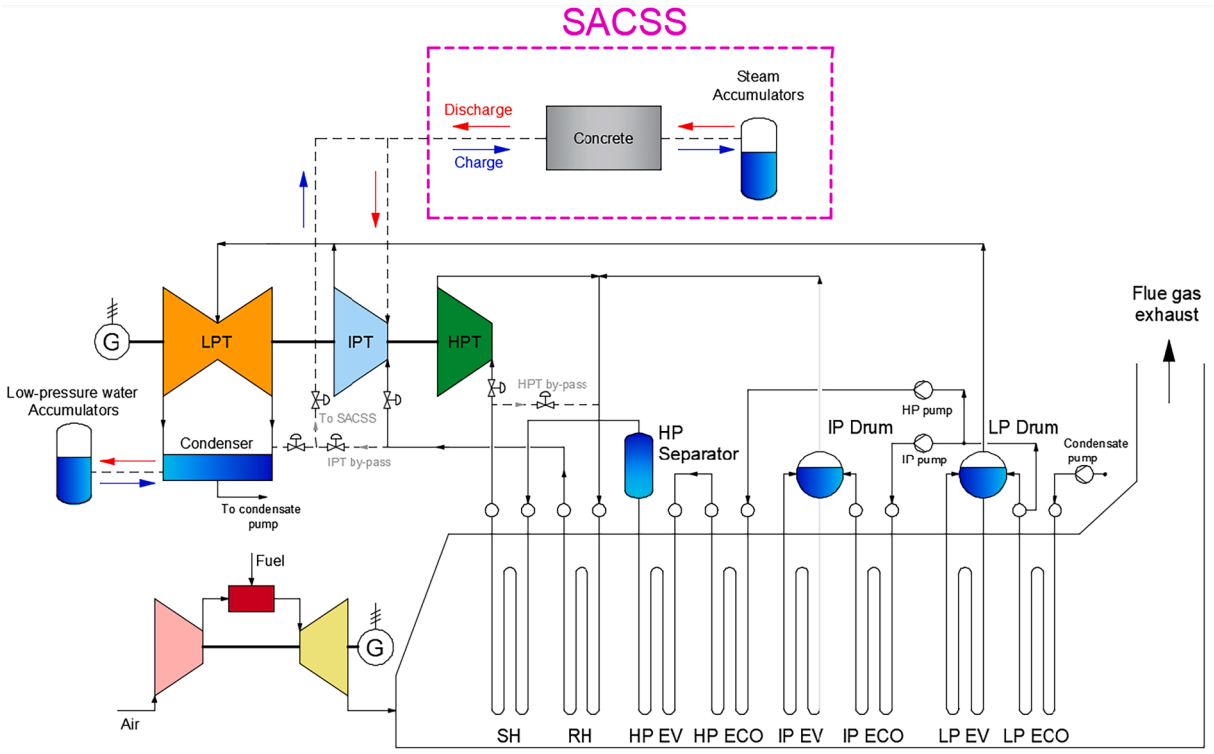

Fig. 1. Schematic of a combined cycle plant with a Benson-type HRSG and SACSS.

operation type. First, the main processes responsible for the efficiency loss of CCP plants, i.e. startups and turbine trips, are analyzed in order to determine the potential amount of energy recoverable by SACSS. Second, a transient thermal model for SACSS is proposed and validated against data of the literature to fairly reproduce the dynamic performance of the system. The discharge operation of SACSS is coupled with a part-load steam turbine model to estimate the generated electricity from the stored energy. Lastly, an economic optimization analysis is performed to maximize the net present value of the SACSS. A sensitivity analysis is performed on four design variables of the SACSS: number of steam accumulator units, accumulating pressure, concrete-block length and outer concrete diameter.

2. Plants selected for the study and steam accumulator and concrete storage system (SACSS) performance description

In this work two plants are selected for the study: i) a CCPP adapted to fast startups using a Benson-type HRSG, ii) a CCPP operated with conventional startups which employs a typical drum-type HRSG. In this section the first case will be presented in detail, since it is considered the most relevant due to the benefits offered by SACSS. Nevertheless, details about the technical and startup data of the second case are shown in Appendix A.

The main technical data of the first case are summarized in Table 1. The highest potential of SACSS will be obtained for those CCPPs using modern gas turbines which can reach 100 % of their nominal load in approximately 20 min independently of hot, warm or cold startup [13]. Those turbines can be mounted with Benson-type HRSGs since they do not have a high-pressure steam drum and therefore can withstand higher ramp rates from gas turbines than conventional drum-type HRSGs.

A schematic of the Benson-type HRSG integrating SACSS is illustrated in Fig. 1. During the startup, both the superheated and reheated steam flows are slowly sent at the steam turbine owing to the ramp-up restrictions while the rest is bypassed directly to the condenser [14]. Fig. 2 shows the most appealing parameters evolution during the fast cold startup of the Benson-type HRSG based on the data from Alobaid et al. [5]. In addition, in the Appendix A, the Fig. A.1 illustrates the hot startup based on measured data about a CCPP employing a conventional drum-type HRSG. Steam flow from the reheater to the condenser is developed as exhibited, as well as the temperature and pressure. Besides, mass flow rate directed to the steam turbine, which delimits the energy recoverable by SACSS, is also exposed in both figures.

The whole reheat steam mass flow typically sent to the condenser during the startup (see Fig. 2 and Fig. A.1) can be stored if SACSS is installed. During the charge of SACSS, firstly, the reheated steam is cooled down in the concrete-block, and secondly, the steam that exits

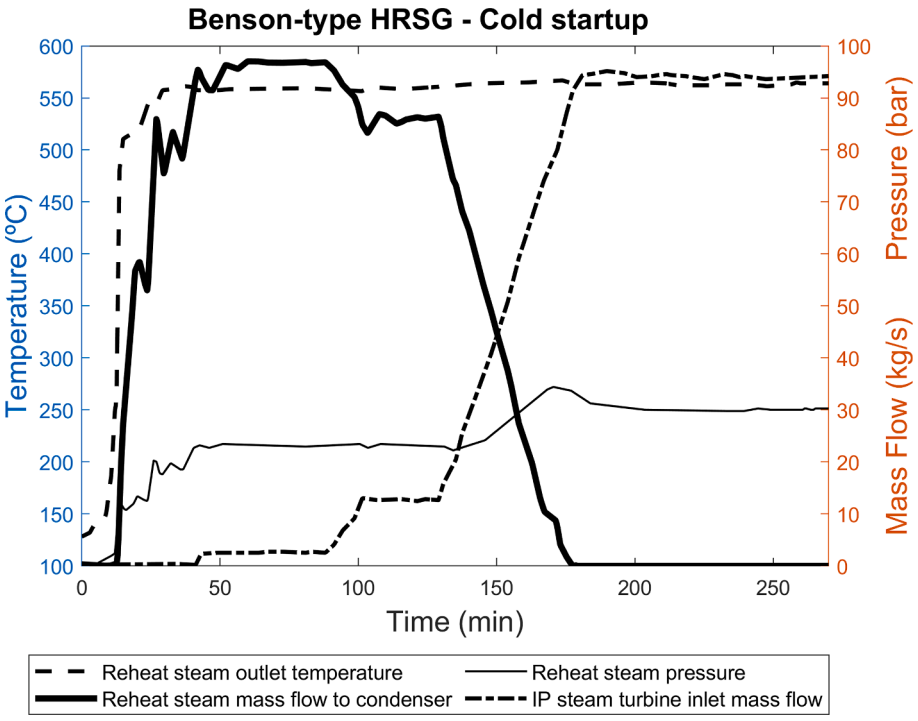

Fig. 2. Turbine boundary conditions and reheater mass flow rate behavior during a fast cold startup of a Benson-type HRSG [5].

Table 2
Estimation of the energy lost during fast startups and steam turbine trips.

	Steam turbine trips	Hot	Warm	Cold
Energy lost during startups (MWh) [5]	44.2[b]	44.2[a]	87.1[a]	237.1[a]
Number of annual events (-) [35]	8	167	10	43

[a] Estimation of the extra energy generated by the steam turbine if the inlet constraints are not considered during the startup.
[b] Steam turbine trips have been energetically accounted as hot startups.

the concrete-block is stored in the steam accumulators. During the discharge of SACSS the steam stored in the steam accumulators is sent to the concrete-block to provide superheated steam and hence reaching the necessary steam conditions to operate the steam turbine efficiently. Other possible use of SACSS consists of discharging part of the steam stored to preheat the HRSG in order to reduce the startup time.

Table 2 exhibits the energy lost for different fast startup cases: hot, warm and cold. These results were calculated using the data from Alobaid et al. [5].

Decreasing the high temperature difference between the exhaust gases and the water along the HRSG constitutes the second purpose of the SACSS. This is why the thermal fluid accumulated could be employed to preheat the heat exchangers before the gas turbine startup. It might be highlighted that forced stops due to HRSG failures are the most likely events due to the constant exposition against thermal stress variations and fatigue damaging, bringing large economic losses [1]. Even though electricity generation seems to be the main profit, thermal preheating may have a strong impact on the economic viability of the plant as well. Effectively, if the fatigue failures are diminished, the forced stops are consequently reduced. It is noteworthy that one day without operation brings an average loss of revenues of 100.000 € for a 400 MWe CCPP. On the other hand, preheating could reduce the maintenance costs in HRSG due to the reduction of the cold and warm startups [36].

Other possible benefits from SACSS consist of suspending the extraction from the LP-turbine to deaerator increasing in this way the power output of steam turbine. The SACSS could provide the saturated steam (or slightly superheated) to deaerator in order to keep suitable quality levels in the water cycle (free of O_2, CO_2, etc).

Table 3
High-alumina concrete-block specifications.

Parameter	Value
Tube outer diameter, d_t (m)	0.025
High-alumina concrete outer diameter, d_c (m)	0.08
Block length, L (m)	28
Number of tubes, N_t	1310
Material tubes	SA-213 T22
High-alumina concrete density, ρ (kg/m^3) [34]	2400
High-alumina concrete specific heat, c_p (J/kg K) [34]	980
High-alumina concrete thermal conductivity, k (W/m K) [34]	2
Insulation material	Rockwool (alumina-silica)
Insulation thermal conductivity, k_{ins} (W/m K) [41]	0.10
Insulation thickness, t_{ins} (m)	1.2

3. Methods

3.1. Concrete model for sensible heat storage

High-alumina concrete constitutes an economical option as a “solid” material to save sensible heat at high temperatures (greater than500 °C) [34]. The good relationship between its density, specific heat capacity and thermal conductivity enables it to become a great thermal booster.

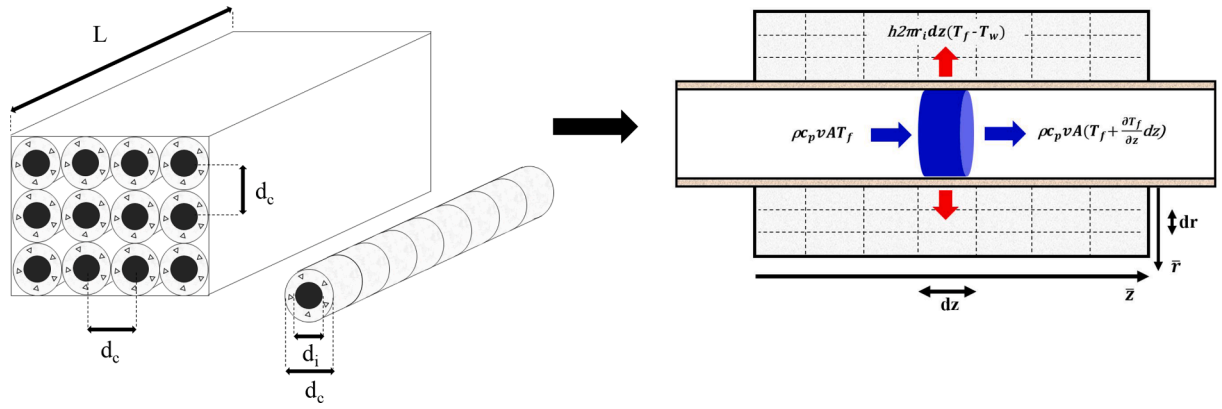

Fig. 3. Diagram of concrete-block configuration and energy balance [42].

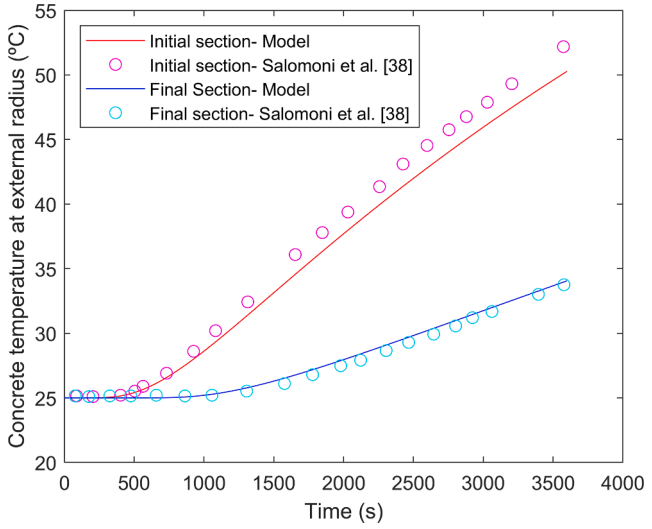

Fig. 4. Model validation during the charge of concrete based on data extracted from [38].

Table 4
Steam accumulator specifications.

Parameter	Value
Number of steam accumulators (units)	8
Steam accumulator useful volume (m^3/unit)	197
Steam accumulator internal diameter (m)	2.5
Initial water volume ratio (%)	70
Design pressure (bar)	25
Mass flow rate (kg/s)	0–89.6
Material	SA-533-Gr B (Carbon steel)

In this sense, high-alumina concrete-blocks are employed in SACSS as a superheater. The use of concrete as a thermal energy storage medium is not new, in fact in the literature can be found in different projects which have worked on this idea [37,38]. In this study, the concrete-blocks in the shape of cylinders are disposed concentrically to the tubes forming a bundle able to effectively absorb and release heat. The tube outer diameter is selected according to similar projects [39]. The tube material is chosen to be the same as reheater tubes of HRSGs [40]. The main measurements and properties of the high-alumina concrete-block are collected in Table 3.

The concrete-block model has been discretized along the tubes axial direction to solve the energy conservation equation and considering one-dimensional and homogeneous flow model as shown in Equation (1). Fig. 3 illustrates the heat exchange process by convection between the fluid and the tube inner surface as well as the concrete-blocks configuration and discretization.

$$\rho c_p v A \frac{\partial T_f}{\partial z} - h2\pi r_i \left(T_f - T_w\right) = \rho c_p A \frac{\partial T_f}{\partial t} \tag{1}$$

The system is supposed to be perfectly insulated during the charge and discharge processes. The thermal resistance of the metal tube wall is neglected and then the temperature at the internal surface of the concrete is the same of the tube [43]. The thermodynamic properties of the steam (i.e. specific heat capacity, density, conductivity and viscosity) are recalculated at every time step, according to the corresponding temperature and pressure. On the other hand, the concrete physical properties remain constant along the procedure. The temporal intervals are calculated to meet Courant's condition. The convective coefficient between the heating fluid and the block is ruled by Gnielinski correlation [44]. The pressure drop along the concrete is accounted since high fluid velocities have been established so as to improve the heat transfer. The maximum velocity of the steam must be limited to prevent noise or vibration problems [45]. The Equation (2) (from Ref. [45]) is evaluated at the steam accumulators design pressure and the average steam temperature along the concrete-block length, i.e. p = 25 bar and T ~ 335 °C, obtaining a maximum velocity of $v_{s,max}$ ~ 66 m/s. However, to reduce the pressure drop and increase the margin of safety, a reduction factor of 2 is used, obtaining a maximum design velocity of: $v_{s,design} = v_{s,max}/2 =$ 33 m/s. As the steam velocity is limited to this value, the number of tubes disposed in parallel is calculated to be 1310.

$$v_{s,max} = 175\left(\frac{1}{\rho_s}\right)^{0.43} \tag{2}$$

The concrete cylinder is radially and axially discretized to capture conveniently the temperature gradients in both directions. The heat conduction equation and the boundary conditions used are displayed through Equations 3–6:

$$\frac{\partial^2 T}{\partial r^2} + \frac{1}{r}\frac{\partial T}{\partial r} + \frac{\partial^2 T}{\partial z^2} = \frac{1}{\alpha}\frac{\partial T}{\partial t} \tag{3}$$

$$\left.\frac{\partial T}{\partial r}\right|_{r=r_o} = 0 \tag{4}$$

$$-k\left.\frac{\partial T}{\partial r}\right|_{r=r_i} = h\left(T_f(z,t) - T(z,r_i,t)\right) \tag{5}$$

$$\left.\frac{\partial T}{\partial z}\right|_{z=0,L} = 0 \tag{6}$$

Finally, the concrete model has been checked against data available in Salomoni et al. [38], whose geometry consists of a 400 m length and 65 mm outer radius concrete tube. Fig. 4 displays the temporal evolution

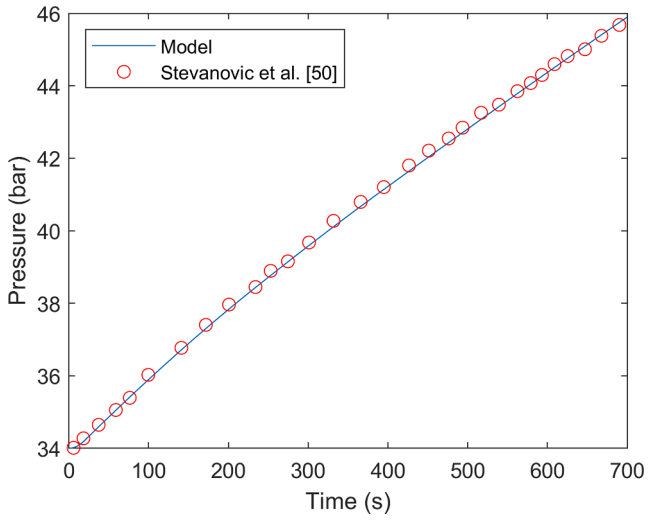

Fig. 5. Model validation during the charge of the steam accumulator based on data extracted from [50].

of the temperature at the outer concrete radius during the charging operation. The mean absolute percentage error (MAPE) of the results shown in Fig. 4 are 2.68 % and 0.98 % for the initial and final section, respectively. Equations (1)–(6) were solved in Matlab by means of an implicit time scheme.

3.2. Steam accumulator model

Steam accumulation is an effective way of thermal energy storage and it has been used especially in projects of concentrating solar power industry [46]. However, the steam accumulation concept may be penalized economically if the storing pressure is high enough due to the high cost of the pressure vessel tank. Other important disadvantage of the steam accumulation storage system is related to the discharge process, in which the gradual reduction of the pressure imposes to the steam turbine to work at part-load conditions, reducing in this way the efficiency conversion from thermal to mechanical energy. A steam accumulator size of 197 m^3/unit is selected [39]. A 2.5 m internal diameter of the steam accumulator was selected to satisfy standard measurements [47]. Carbon steel SA-533-Gr B is selected due to the high allowable stress compared with other typical pressure vessels materials [48]. This permits a reduction of the wall thickness, weight and cost of the steam accumulator. The main design parameters of the steam accumulators considered in this work are summarized in Table 4.

A second order model proposed by Aström and Bell [49] has been selected to describe the dynamic response of the steam accumulators. It provides accurate results of the transient evolution of the two main thermodynamic variables of the steam accumulators, i.e. the pressure and the total water volume. The model assumes thermodynamic equilibrium between steam and water, and thus they have the same saturated temperature and pressure. No heat losses are considered during the time the steam is being saved. Furthermore, it may be noticed that both incoming and outgoing mass flow rates depend on pressure and hence uncoupled models are related. The model has been solved numerically by using Runge-Kutta method on the basis of initial values of dependent variables, fluids flow rates and enthalpies as well as steam accumulator pressure. The software used to perform the calculations was Matlab. The modeling is mainly based on the mass and energy balances concerning about the internal volume contained in the steam accumulators as shown in Equations (7)–(8).

$$\frac{dM}{dt} = \dot{m}_l + \dot{m}_s \tag{7}$$

$$\frac{dH}{dt} = (\dot{m}_s h_s) + (\dot{m}_l h_l) + V\frac{dp}{dt} \tag{8}$$

The usage of this model brings reliable results of the physical response for changes either in the inlet/outlet feedwater flow rate or in the steam flow rate. The validation of the system performance has been carried out through direct comparison between pressure development from the simulation and the data extracted from [50]. The case represents the charging procedure of a steam accumulator as exhibited in Fig. 5. The comparison between the model and the results from [50] obtains a MAPE of 0.1702 %. The pressure growth closely aligns the referred one and therefore, the accuracy of the recreation is verified and meets the desired requirements.

3.3. Steam turbine model

When the charging period is completed, the steam is kept in the steam accumulators and thus it becomes available to generate electricity. To determine the steam turbine power output during the discharge process, the part-load behavior of the turbine must be modeled since the inlet mass flow rate, temperature and pressure vary during the process. As generating electricity, no further steam or heat is utilized, just the saved fluid and heat stored in the concrete. Turbine isentropic efficiency, whose nominal value is considered 93 %, varies according to Equations (9–10) [51]:

$$Reduction(\%) = 0.191 - 0.409\left(\frac{\dot{m}_s}{\dot{m}_{s,0}}\right) + 0.218\left(\frac{\dot{m}_s}{\dot{m}_{s,0}}\right)^2 \tag{9}$$

$$\eta_t = \eta_{t,0}(1 - Reduction(\%)) \tag{10}$$

The mass flow rate evolution over a turbine stage is ruled by means of Stodola's law as expressed in Equation (11):

$$\dot{m}_s = K_{st}\frac{p_s}{\sqrt{T_s}} \tag{11}$$

Lastly, the power output of the steam turbine is obtained according to Equation (12). Additionally, Equation (13) is used to evaluate the recovery efficiency in the process, which is defined as the relation between the energy generated during the discharging process and the energy generated by the turbine if the low-pressure steam is not bypassed to the condenser during the startup.

$$W_t = \dot{m}_s(h_{in} - h_{out}) \tag{12}$$

$$\eta_{rec} = \frac{\int_0^{t_{dis}} W_t dt}{E_{max}} = \frac{E_{gen}}{E_{max}} \tag{13}$$

3.4. Economic analysis

The cost estimation of SACSS becomes fundamental so as to determine the viability of the project. The pressurized components as the tubes and steam/water accumulators of the system must be sized to withstand thermal and mechanical loads. The thicknesses have been calculated using ASME rules as follows [52]:

$$t = p\frac{d/2}{S{\cdot}E - 0.6{\cdot}p} \tag{14}$$

Table 5
Variables of the economic analysis for the exposed scenario.

Parameter	Value	Ref.
Mean selling price of electricity (€/MWh)	58.33	[20]
Number of years, N_y (years)	20	[20]
Annual interest, i (%)	6	[20]
Carbon credits price (€/tonCO_2)	47.17	[55]
Inflation rate, θ (%)	3	[56]

where p is the internal pressure, d is the outer diameter, E is the joint efficiency factor and S is the maximum allowable stress evaluated at the maximum working temperature.

Attending to the main components involved in this work, the most expensive ones are the steam and the low-pressure water accumulators. They are considered as pressure vessels and characterized economically considering ladders, platforms and a nominal number of nozzles and manholes [53]. The method is given by:

$$C_T = F_M C_V + C_{LP} \tag{15}$$

where F_M denotes the material factor (equal to 1 for carbon steel), C_V is based on the weight of the accumulators and C_{LP} is an added cost for ladders and platforms. The last two are defined as:

$$C_V = e^{\left(8.9552 - 0.2330[ln(M_V)] + 0.0433[ln(M_V)]^2\right)} \tag{16}$$

$$C_{PL} = 2.005(d_i)^{(0.20294)} \tag{17}$$

Finally, both tubes and concrete costs are dependent on the amount of material. As ASTM A213 tubes are accounted, a price of 2.57 €/kg has been established (originally, 1.67 €/kg for India but arranged for European destination) [54]. The price of the high-alumina concrete is 151 €/m^3 according to [34].

Once the overall costs are determined, the income from electricity sale is considered and thus the profitability of the system is studied. The main parameters which define this study are the payback period and the net present value (NPV). The first one establishes when the inversion is amortized. Meanwhile, the second one shows the difference between the present value of cash inflows and the present value of cash outflows over a temporal period, being obtained as depicted in Equation (18).

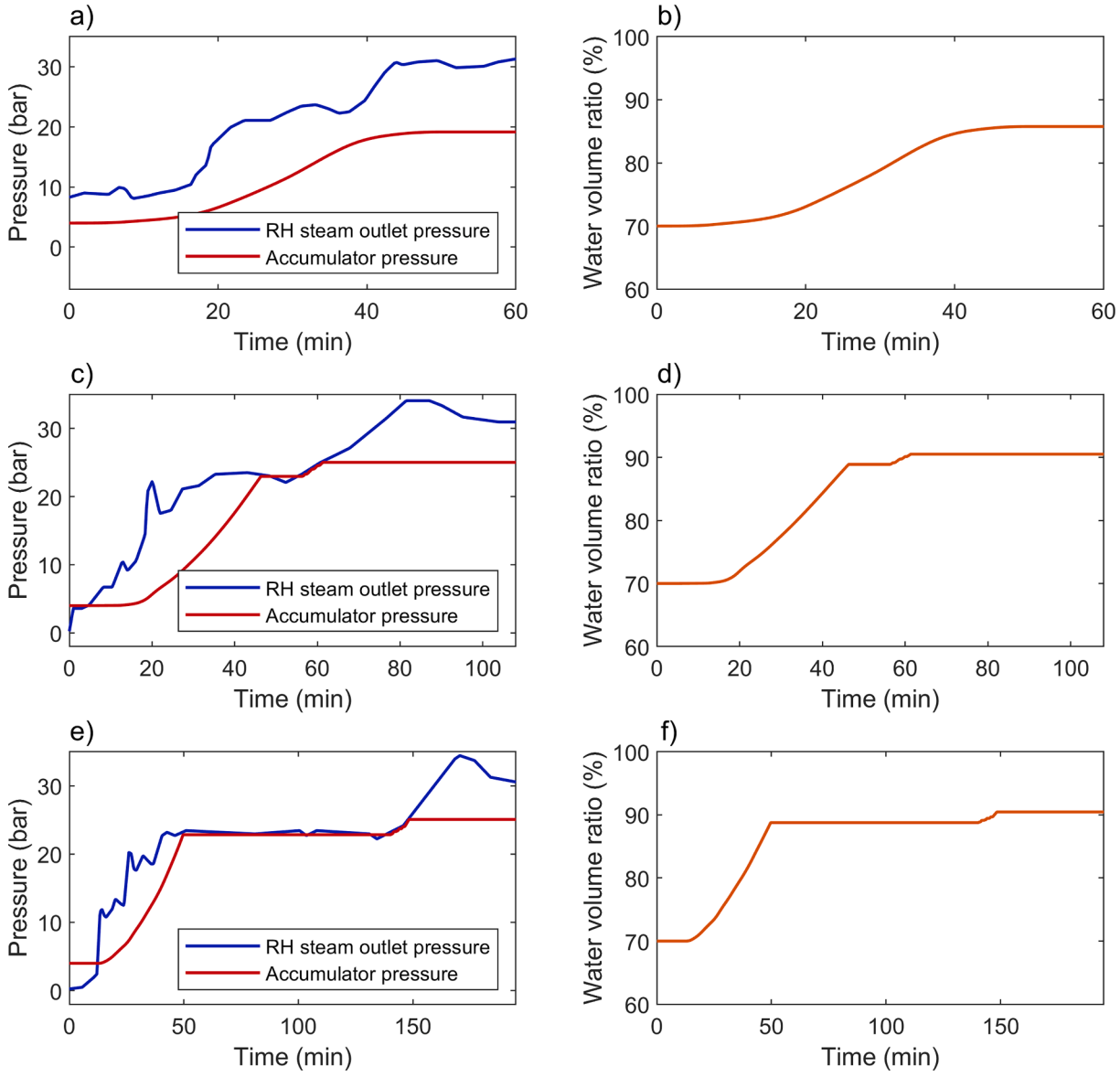

Fig. 6. Charging process of the steam accumulators during: a) b) hot startup, c) d) warm startup and e) f) cold startup.

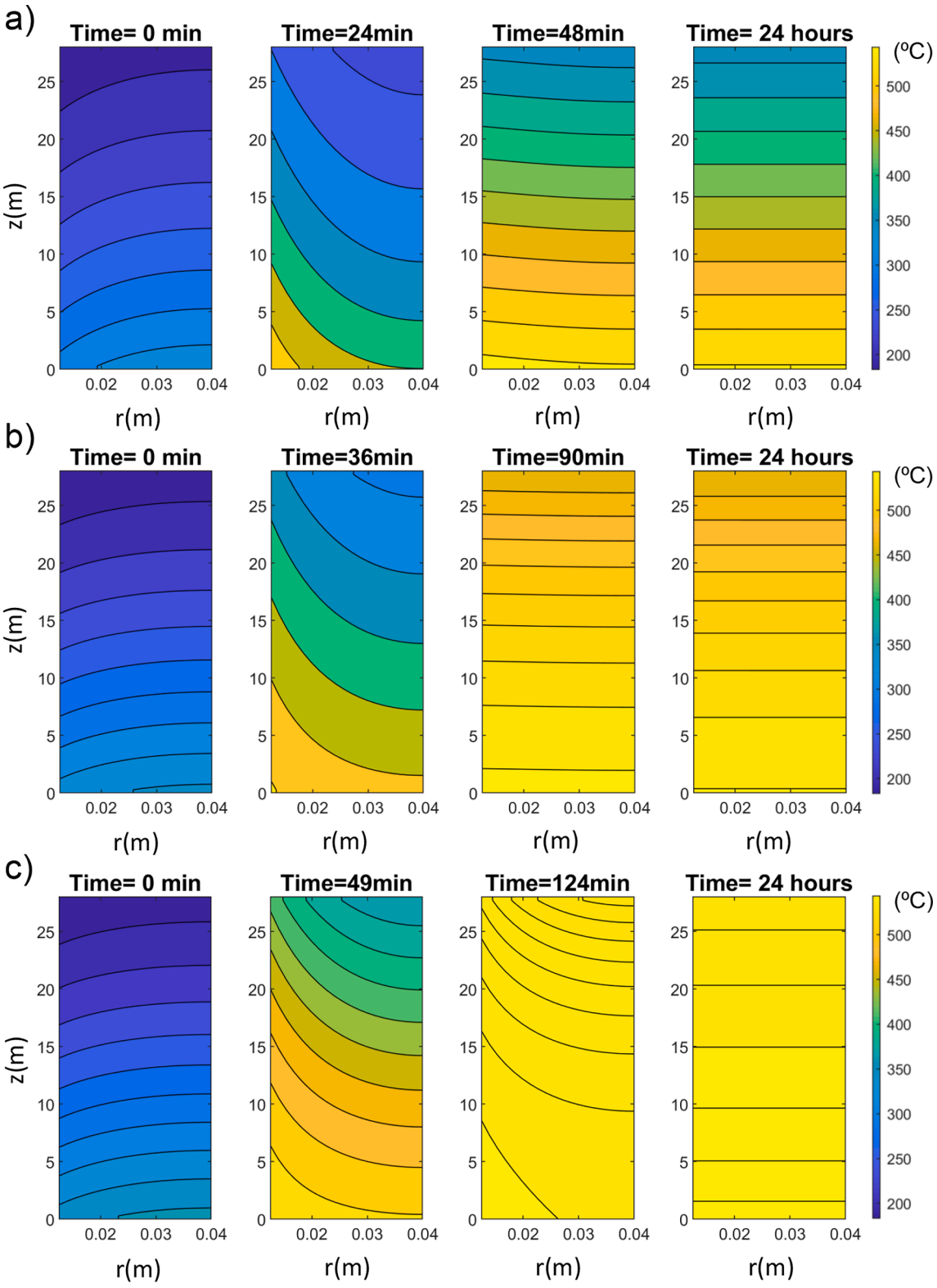

Fig. 7. Temperature profile of the concrete-block for charging process obtained from: a) hot startup, b) warm startup and c) cold startup.

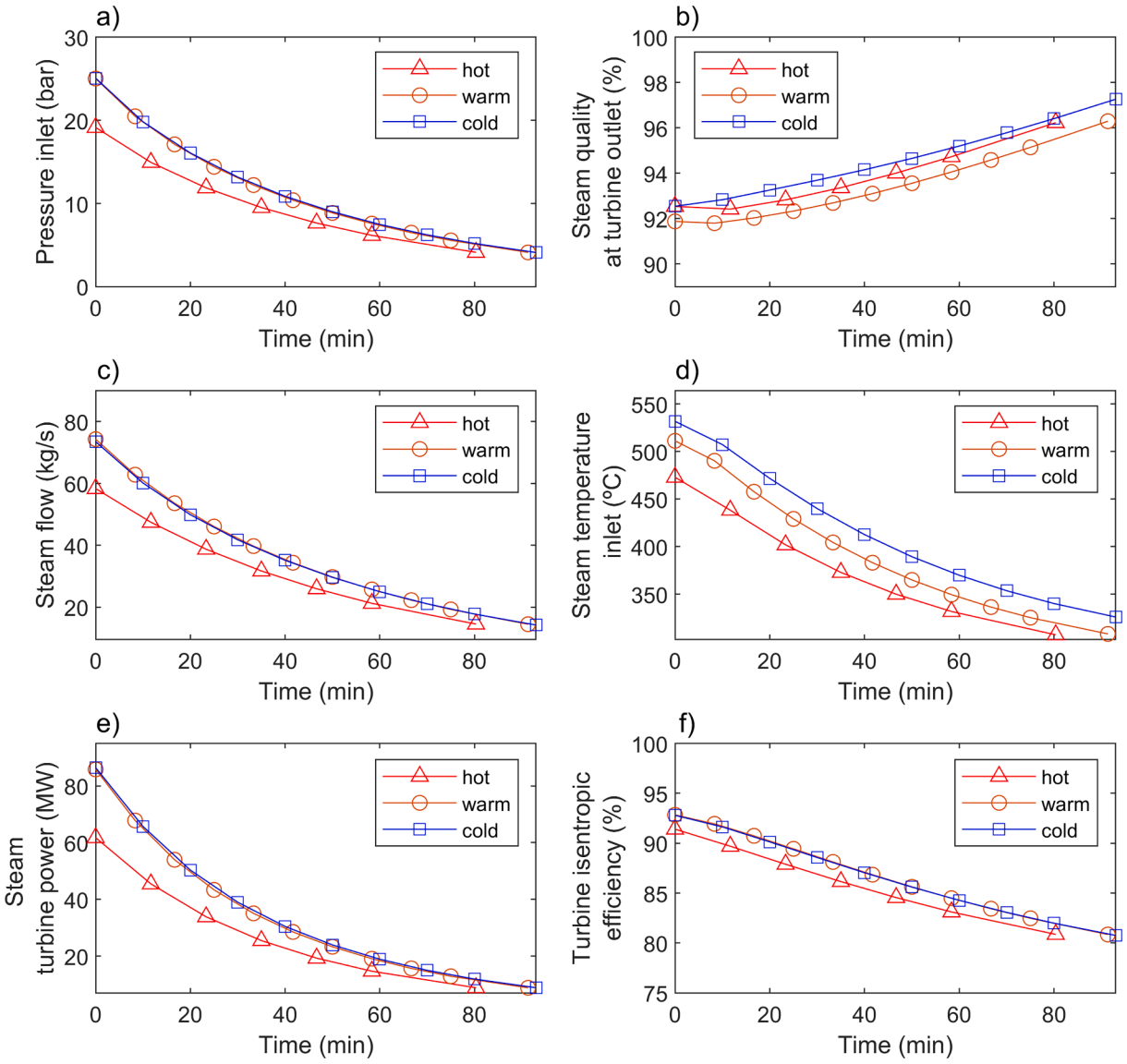

Fig. 8. Steam turbine performance during the discharge of SACSS: a) steam turbine inlet pressure, b) outlet steam quality, c) steam mass flow rate, d) steam inlet temperature, e) turbine power and f) isentropic efficiency.

Table 6
Thermodynamic simulation results during the discharge for every startup.

Startup	Hot	Warm	Cold
Energy generated, E_{gen} (MWh)	35.6	49.5	50.8
Recovery efficiency, η_{rec} (%)	80.4	56.8	21.4
Minimum steam quality, x_{min} (-)	0.924	0.917	0.925

$$NPV = -I_0 + \sum_{n=1}^{N_y} \frac{F_n}{(1+i)^n} \tag{18}$$

The *NPV* has been evaluated through the following variables: i) mean selling price of electricity (€/MWh), ii) lifetime (years), iii) interest rate *i*. Table 5 collects the values used for the economic analysis which have been obtained from similar projects [20].

One main advantage of the SACSS implementation is that electricity generation does not release greenhouse gases. Thus, potential benefits coming from carbon credits might be accounted. According to the Spanish Ministry for Ecological Transition and the Demographic Challenge (MITECO) and considering an average cycle efficiency of 50 %, the emission factor of CCPPs (f) is 0.404 $kgCO_2/kWh$ [57]. Then, carbon dioxide saving might be determined from annual electricity generation (E_{gen}) provided by SACSS. Regarding the price of carbon credits (P_c), a value of 47.17 €/$tonCO_2$ is considered as it comprises the mean auction value in 2021 [55]. This value has experienced a vertiginous growing along the last few years, ranging from 5.83 €/$tonCO_2$ to 24.84 €/$tonCO_2$ in 2019. Consequently, it is supposed that carbon credits price annually increases owing to inflation rate (θ), considered equal to 3 % [56]. Finally, annual income resulted from carbon credits in the n^{th} year can be obtained as follows:

$$B_c^n = f E_{gen} P_c (1+\theta)^{n-1} \tag{19}$$

4. Results and discussion

In this section are presented the results of this work together with a

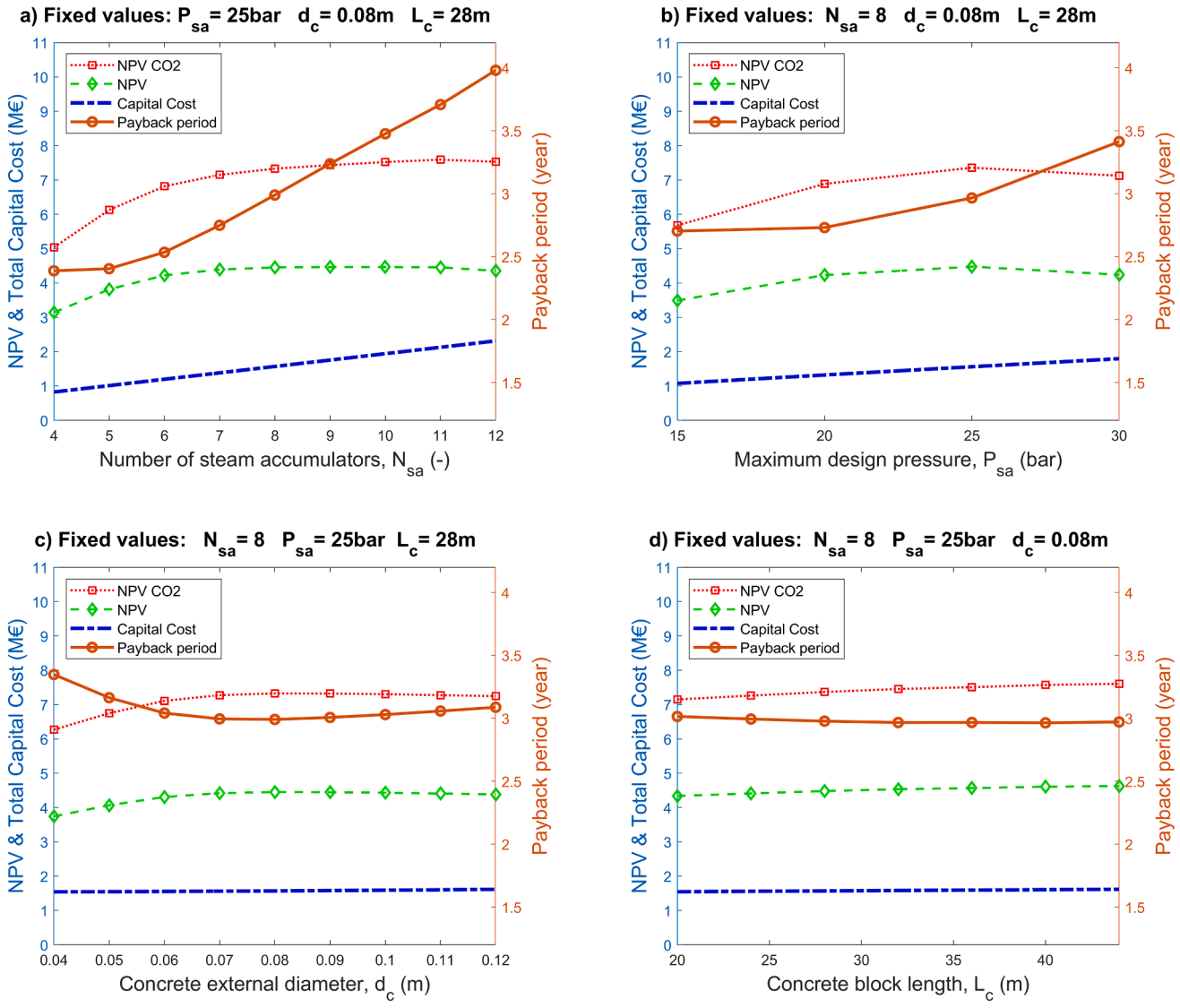

Fig. 9. Economic analysis results a) number of steam accumulators b) accumulating pressure c) concrete outer diameter d) concrete-block length.

Table 7
SACSS performance integrated into a CCPP operated with conventional startups.

Startup	Hot	Warm	Cold
Energy generated, E_{gen} (MWh)	22.17	29.3*	29.3*
Recovery efficiency, η_{rec} (%)	76.5	–	–
Minimum steam quality, x_{min} (-)	0.903	0.934*	0.934*

*Estimated considering that the SACSS is fully charged.

Table 8
Economic results of the SACSS integration into a CCPP operated with conventional startups.

Parameter	Value	Variation respect a CCPP operated with fast startups
Total capital cost (M€)	1.06	−33 %
Payback period (years)	3.4	+13 %
NPV (M€)	2.53	−43 %
NPV CO2 (M€)	4.16	−43 %

brief discussion. They have been divided into three subsections: i) the thermodynamic results about the operations of charging and discharging of SACSS, ii) the results of the economic analysis about the integration of SACSS into a CCPP able to execute fast startups, iii) the results of the economic analysis about the integration of SACSS into a CCPP operated with conventional startups.

4.1. Thermodynamic results

In this section, the thermodynamic results about the integration of SACSS into a CCPP adapted to fast startups will be presented in detail, since it is considered the most relevant due to the benefits offered by SACSS. However, details of thermodynamic results about the integration of SACSS into a CCPP operated with conventional startups are shown in Appendix A.

The charging process is carried out using the available low-pressure steam sent to the SACSS (see Fig. 1) instead of by-passing to the condenser while a startup is taking place. The simulation results during the charging mode are exhibited in Fig. 6. The charging process starts at the minimum accumulation pressure, i.e. 4 bar, and finishes at the maximum design pressure value, i.e., 25 bar, for warm and cold startup cases (Fig. 6.c/e). For the hot startup case (Fig. 6.a), the maximum

design pressure is not achieved being the maximum accumulation pressure of 19 bar.

Fig. 7 shows the temperature fields of the concrete-block during the charging process. The maximum storing period has been set to 24 h, which is a reasonable approach for a CCPP with a regular cycling service operation-type. A conservative heat transfer analysis reveals that during 24 h the heat losses are not significant obtaining a maximum temperature drop around 2.2 °C/day (see Fig. 7). Additionally, the temperature drop due to the axial temperature gradient has been also analyzed, being around 1.8 °C/day for the hot startup case (Fig. 7.a) and negligible for the warm and cold cases (Fig. 7.b/c).

The simulation results of the discharging process are depicted in Fig. 8, where the main parameters shown are: turbine inlet pressure, turbine inlet steam mass flow rate, turbine inlet steam temperature, turbine power and steam quality at the turbine outlet. As the inlet pressure (Fig. 8.a), temperature (Fig. 8.d) and mass flow rate (Fig. 8.c) of steam decrease with the time, the steam turbine gradually reduces the power output (Fig. 8.e). Thanks to the heat absorbed by the concrete-blocks during the charge mode, the steam can be heated from the saturated steam up to temperatures close to the nominal steam turbine inlet (~550 °C) during the discharge (see Fig. 8.d). An important consideration to operate the steam turbine safely is to assure a steam quality x greater than 84 %, otherwise the turbine paddles can be eroded by water droplets formation [58]. As can be seen, this requirement is largely satisfied since the minimum steam quality during the process is higher than 91 % for the startup cases (Fig. 8.b). The discharge process takes around 93 min for warm and cold startup cases, and 80 min for the hot startup case. Please note that the turbine is operated only by using the accumulated steam and the heat contained in the concrete-block, no further energy is employed.

The main results of the discharging process for the different startups are summarized in Table 6. Considering the energy saved by each startup case and the number of startups described in Table 2, an amount of 3 640 tons of CO_2 emissions can be avoided per year thanks to SACSS. According to the initial thermodynamic analysis, the amount of the energy recoverable from hot, warm and cold startups are 44.26, 87.1 and 237.5 MWh, respectively. Opposite to the energy generated, there is a relative high difference compared to the theoretical maximum, especially for the cold case. This effect is directly related with the recovery efficiency ranged between 21.4 % and 80.4 % for the simulated cases. Although the recovery efficiency, which can be improved increasing the amount of concrete and/or the number of steam accumulators, it may be not interesting if it affects negatively to the profitability of the plant. To shed light on that question, the economic impact of the amount of concrete and the number of steam accumulators is analyzed in the following section.

4.2. Economic results for a CCPP adapted to fast startups

An economic sensitivity analysis is conducted to evaluate the profitability of the SACSS integrated within a CCPP. With that aim, two economical parameters have been selected: net present value (NPV) and payback period. Concretely, these parameters are obtained as function of the main design variables: i) number of steam accumulators ii) accumulating pressure iii) concrete outer diameter iv) concrete-block length. The revenues come from the electricity sale, where it was assumed that the startup performance during the entire operation life of the plant does not vary. The results of the economic analysis are shown in Fig. 9, whose optimum solution for SACSS is composed of: 8 steam accumulators, accumulating pressure of 25 bar, concrete diameter equal to 0.08 m and a concrete-block length of 28 m. Despite tube (and concrete-block) lengths larger than 28 provide slightly better results, this value has been selected to satisfy the largest standard measurement according to boiler tube manufacturers [59,60].

Regarding the economic parameters the optimum scenario is defined, displaying the following trends:

- Fig. 9. (a), for a number of steam accumulators larger than 8, the NPV does not present a significant improvement whereas the payback grows at a linear rate. Therefore, the best choice is considered to be 8 steam accumulators with a NPV of 4.45 M€ (7.32 M€ if the benefits from carbon credits selling are considered) and 3 year of payback period;
- Fig. 9 (b), for a design pressure higher than 25 bar, the installation costs increase at higher rate than the benefits, then the profitability decreases;
- Fig. 9 (c), wider concrete diameters bring the best results, where values between 0.07 and 0.08 m provide the lowest payback period (3 years);
- Fig. 9 (d), concrete-block length variations show the smallest sensitivity. Nevertheless, a length of 28 m seems to be the optimum measurement since it is the maximum standard length available according to boiler tube manufacturers [59,60].

The economic analysis about SAACS integrated into a CCPP adapted to fast startups returns optimistic results showing a payback period of only 3 years, NPV equal to 4.45 M€ and installation costs of 1.57 M€. It is worth to mention that the NPV can be increased up to 7.32 M€ if the benefits from carbon credits are considered. Despite unavoidable uncertainties inherent to engineering projects, the low payback period and the significant margin of benefits presented by SACSS makes it a promising solution to increase the profitability of CCPPs operated under cycling conditions.

4.3. Economic results for a CCPP operated with conventional startups

In this section is analyzed from economical point of view the integration of SACSS into a Tirreno Power 390 MW CCPP [14], which employs a conventional drum-type HRSG. Now, the economic analysis of SACSS is supported by actual measured data during the startup phase as can be seen in the Appendix A.

Although current electricity markets with high penetration of variable renewable energies push flexible plants to operate as faster as possible, there is a large amount of active CCPPs which may be not suitable for fast startups (i.e. gas turbine startup from 0 % load to 100 % load in ~ 20 min). In these cases, if the CCPP has not been adapted, the steam turbine bypass system does not have the capacity to evacuate to the condenser the high amount of steam generated in the HRSG during a fast startup [11]. Nevertheless, the amount of steam bypassed through the condenser is still significant, specially vintage F class gas turbines which have a relatively high MECL [11].

According to the thermodynamic results presented in the Appendix A, the energy generated by SACCS is 24 MWhe from the energy recovered from a hot startup based on measured data. The SACSS has been optimized to maximize the energy generated for the hot startup case. Three design parameters of Table 3 and Table 4 have been modified: i) The steam accumulator design pressure is reduced from 25 to 20 bar. ii) The number of steam accumulator units is reduced from 8 to 6. ii) The outer concrete diameter is modified from 0.08 m to 0.06 m. Unfortunately, measured data of warm and cold startups of Tirreno Power CCPP

are not available. An extrapolation of the energy recoverable by SACSS for warm and cold startup cases is made considering that SACSS is fully charged after in each startup process. The main thermodynamic results about the integration of SACSS into a CCPP operated with conventional startups are summarized in Table 7.

The most relevant economic results about the integration of SACSS into a CCPP operated with conventional startups are displayed in Table 8. As it can be seen, the payback period is increased about 13 % compared to the CCPP operated with fast startups. Despite the lower energy generated by SACSS in the case of a CCPP operated with conventional startups, the capital cost reduction about 33 % keeps the payback period below of 4 years. On the other hand, a reduction of 43 % is obtained for the NPV and the NPV considering the benefits from CO_2 credits. Finally, the estimation of the emissions avoided integrating SACSS into a CCPP with a conventional drum-type HRSG case are estimated to be around 2 175 tons of CO_2 per year..

5. Conclusions

In this paper, a novel storage Steam Accumulator and Concrete Storage System (SACSS) was presented to recover energy typically lost during startups in combined cycles. Two different scenarios were considered for the economic analysis: a combined cycle power plant (CCPP) adapted to fast startups using a Benson-type heat recovery steam generator (HRSG) and a CCPP operated with conventional startups. It is worth mentioning that the second scenario is based on measured data during a hot startup. A preliminary analysis about the CCPP adapted to fast startups revealed losses of energy of 44.2, 87.1 and 237.1 MWh for hot, warm and cold startups, respectively. This energy can be saved by SACSS, and it can be used to generate electricity or to preheat the HRSG in order to reduce its fatigue damage during fast startups. Dynamic thermal models have been developed and validated against data from literature to reliably simulate the charging and discharging operations of the SACSS.

The economic optimization of SACSS was performed focusing in four design variables: number of steam accumulator units, storage design pressure, concrete-block length and outer concrete diameter. The main outcomes of the current investigation can be summarized as follows:

- The integration of SACSS into a CCPP adapted to fast startups shows a payback period of 3 years and a net present value of 4.45 M€. The integration of SACSS into a CCPP operated with conventional startups obtains a payback period of 3.4 years and a net present value of 2.53 M€.
- The net present value can be increased in both cases around 60 % if the benefits from carbon credits are included.
- During the discharge of SAACS, the net energy recovered from hot, warm and cold startups for the fast startup case is: 35.6, 49.5 and 50.8 MWh, respectively. These values are reduced around 35 % for the conventional startup case.
- During the discharge process the steam quality at the low-pressure steam turbine outlet is kept in suitable ranges (greater than90 %) to avoid compromising the structural integrity of the steam turbine.
- The design variable with the highest sensibility on the economic results was the number of steam accumulators due its high cost compared to the high-alumina concrete or the low-alloy tubes.
- The estimation of tons of CO_2 emissions avoided per year, if SACSS is installed, are 3 640 and 2 175, for fast and conventional startup cases, respectively.

To conclude, the integration of the SACSS leads to a better exploitation of CCPPs, which substantially improves the annual energetic efficiency. Additionally, SACSS may help to reduce the forced outage rates due to fatigue failures by means of HRSG preheating.

CRediT authorship contribution statement

P.A. González-Gómez: Conceptualization, Methodology, Software, Writing – original draft, Visualization, Funding acquisition. **M. Laporte-Azcué:** Conceptualization, Methodology, Software, Writing – review & editing. **M. Fernández-Torrijos:** Conceptualization, Methodology, Software, Writing – review & editing. **D. Santana:** Resources, Conceptualization, Writing – review & editing, Supervision, Funding acquisition.

Declaration of Competing Interest

The authors declare that they have no known competing financial interests or personal relationships that could have appeared to influence the work reported in this paper.

Acknowledgments

This research is partially funded by the Spanish government under the project RTI2018-096664-B-C21 (MICINN/FEDER, UE), the fellowship "Ayuda a la investigación en energía y medio ambiente" of the Iberdrola España Foundation, the scholarship "Ayudas para la formación del profesorado universitario" (FPU-02361) awarded by the Spanish Ministerio de Educación, Cultura y Deporte (MECD), and the fellowship "Programa de apoyo a la realización de proyectos interdisciplinares de I + D para jóvenes investigadores de la Universidad Carlos III de Madrid 2019-2020" under the project ZEROGASPAIN-CM-UC3M (2020/00033/002), funded on the frame of "Convenio Plurianual Comunidad de Madrid-Universidad Carlos III de Madrid 2019-2022".

Appendix A. . Technical data and thermodynamic results about the integration of SACSS into a CCPP operated with conventional startups

A.1. Technical data.

Table A1
Technical data of Tirreno Power 390 MW CCPP [14].

HRSG Type	Steam conditions				Steam turbine power	Gas turbine power
Drum-typeTriple pressure	**HP**	**RH/IP**	**LP**	**Condenser**		
	p = 124 bar	p = 34 bar	–	p = 0.056* bar	120 MW	270 MW
	T = 550 °C	T = 550 °C	–			
	$\dot{m}$ = 70 kg/s	$\dot{m}$ = 86 kg/s	–			

* The condenser pressure is not available in [14], a typical condenser pressure of CCPP has been considered.

A.2. Measured data during the hot startup.

Fig. A1 shows measured data during the hot startup of Tirreno Power 390 MW CCPP [14].

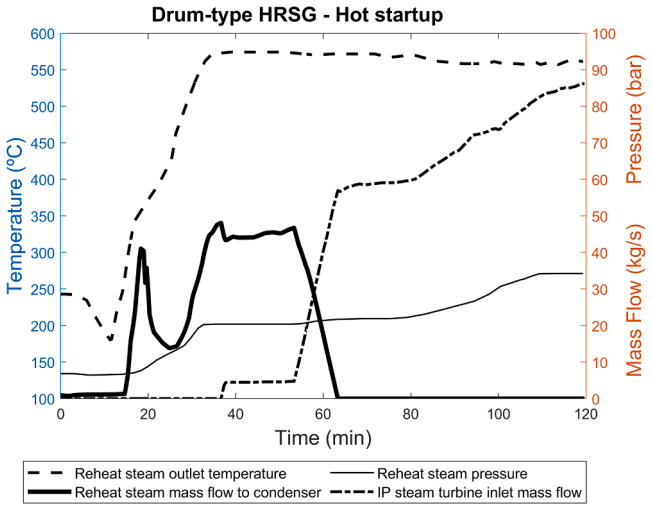

Fig. A1. Measured data during a hot startup of Tirreno Power 390 MW CCPP from Rossi et al. [14].

A.3. SACSS design specifications.

The main design parameters used for the case of a CCPP operated with conventional startups are shown in Tables A.2 and A.3.

Table A2
High-alumina concrete-block specifications.

Parameter	Value
Tube outer diameter, d_t (m)	0.025
High-alumina concrete outer diameter, d_c (m)	0.06
Block length, L (m)	28
Number of tubes, N_t	1310
Material tubes	SA-213 T22
High-alumina concrete density, ρ (kg/m^3) [34]	2400
High-alumina concrete specific heat, c_p (J/kg K) [34]	980
High-alumina concrete thermal conductivity, k (W/m K) [34]	2
Insulation material	Rockwool (alumina-silica)
Insulation thermal conductivity, k_{ins} (W/m K) [41]	0.10
Insulation thickness, t_{ins} (m)	1.2

Table A3
Steam accumulator specifications.

Parameter	Value
Number of steam accumulators (units)	6
Steam accumulator useful volume (m^3/unit)	197
Steam accumulator internal diameter (m)	2.5
Initial water volume ratio (%)	70
Design pressure (bar)	20
Mass flow rate (kg/s)	0–54
Material	SA-533-Gr B (Carbon steel)

A.4. Thermodynamic results.

The thermodynamics results of the SACSS integrated into a CCPP operated with conventional startups are shown in Figs. A.2 and A.3 for the charging process, and Fig. A.4 for the discharging process.Fig. 9.

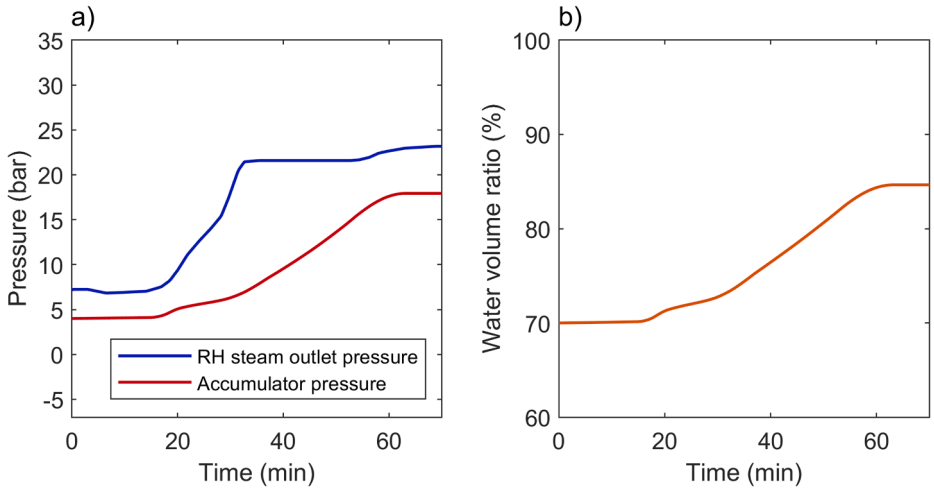

Fig. A2. Charging process of the steam accumulators during the hot startup.

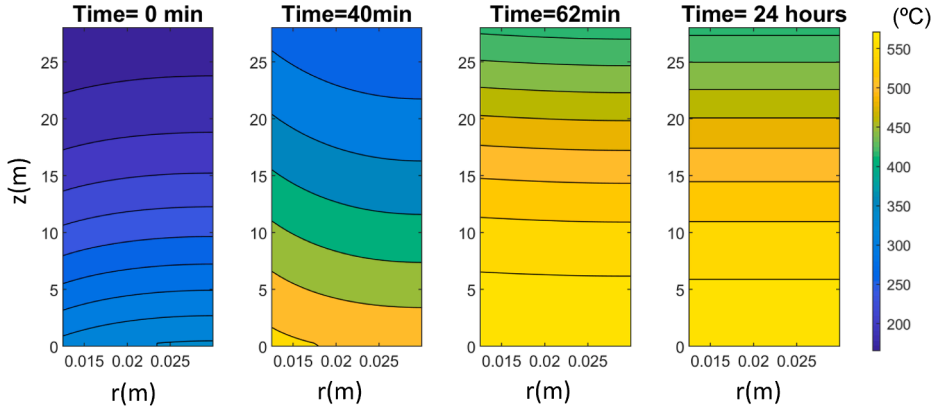

Fig. A3. Temperature profile of the concrete-block during the charging process.

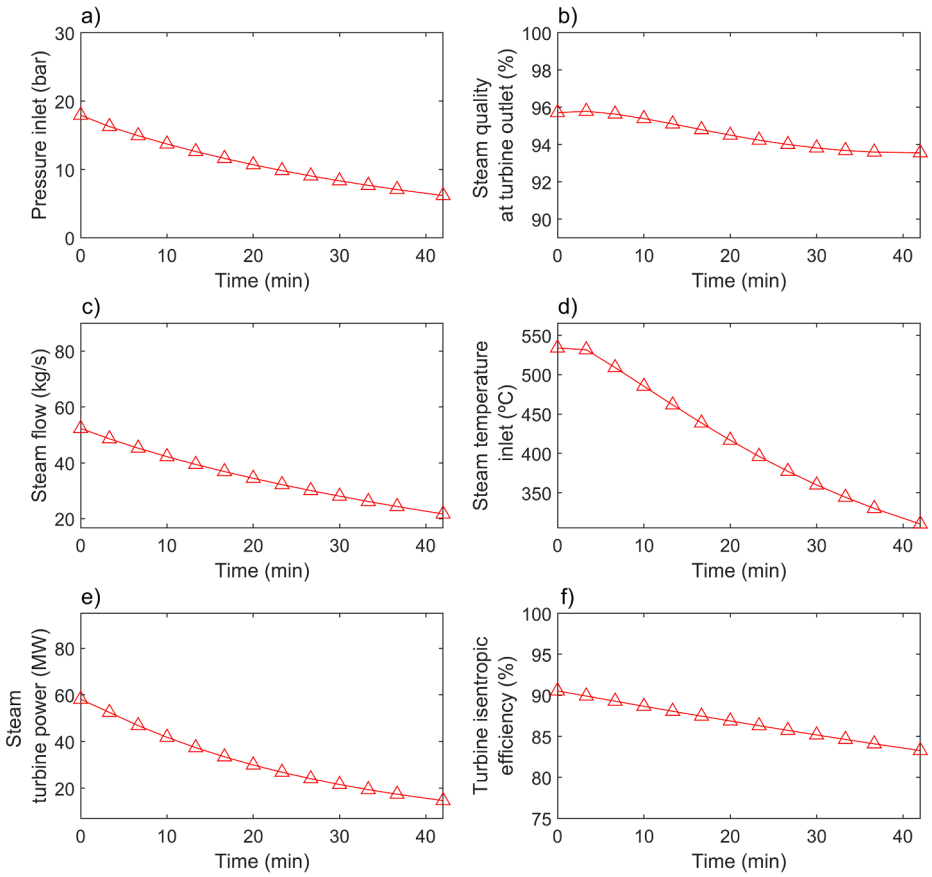

Fig. A4. Steam turbine performance during the discharge of SACSS: a) steam turbine inlet pressure, b) outlet steam quality, c) steam mass flow rate, d) steam inlet temperature, e) turbine power and f) isentropic efficiency.

References

[1] Wogrin S, Galbally D, Ramos A. CCGT unit commitment model with first-principle formulation of cycling costs due to fatigue damage. Energy 2016;113:227–47. https://doi.org/10.1016/j.energy.2016.07.014.

[2] Ferreira HL, Garde R, Fulli G, Kling W, Lopes JP. Characterisation of electrical energy storage technologies. Energy 2013;53:288–98. https://doi.org/10.1016/j.energy.2013.02.037.

[3] Victoria M, Gallego-Castillo C. Hourly-resolution analysis of electricity decarbonization in Spain (2017–2030). Appl Energy 2018;233–234:674–90. https://doi.org/10.1016/j.apenergy.2018.10.055.

[4] Tapetado P, Usaola J. Capacity credits of wind and solar generation: The Spanish case. Renew Energy 2019;143:164–75. https://doi.org/10.1016/j.renene.2019.04.139.

[5] Alobaid F, Pfeiffer S, Epple B, Seon C-Y, Kim H-G. Fast start-up analyses for Benson heat recovery steam generator. Energy 2012;46(1):295–309. https://doi.org/10.1016/j.energy.2012.08.020.

[6] Lefton SA, Grimsrud GP, Besuner PM, Agan DD, Grover JL. Analysis of cycling impacts on combined cycle heat recovery steam generators and evaluating future costs of countermeasures to reduce impacts. Proc POWER2008 2008:1–12.

[7] Basañez A, Lorenzo M. The Challenge of Combined Cycle Thermal Plants to the Current Energy Situation. 6th Int Conf Ind Eng Ind Manag; 2012, p. 871–8.

[8] Wojcik JD, Wang J. Feasibility study of Combined Cycle Gas Turbine (CCGT) power plant integration with Adiabatic Compressed Air Energy Storage (ACAES). Appl Energy 2018;221:477–89. https://doi.org/10.1016/j.apenergy.2018.03.089.

[9] Gülen SC. Gas Turbines for Electric Power Generation. Cambridge, UK: Cambridge University Press; 2019.

[10] Hentschel J, Babić U, Spliethoff H. A parametric approach for the valuation of power plant flexibility options. Energy Rep 2016;2:40–7. https://doi.org/10.1016/j.egyr.2016.03.002.

[11] Gülen SC. Gas Turbine Combined Cycle Power Plants. Boca Raton, FL: CRC Press Taylor & Francis Group; 2020.

[12] Siemens. Siemens Benson HRSG 2021. https://assets.siemens-energy.com/siemens/assets/api/uuid:5a0c4ea8-962a-4fa9-93de-1344c82ff9f6/benson-hrsg-171023.pdf (accessed November 2, 2021).

[13] Gonzalez-Salazar MA, Kirsten T, Prchlik L. Review of the operational fl exibility and emissions of gas- and coal- fi red power plants in a future with growing renewables. Renew Sustain Energy Rev 2018;82:1497–513. https://doi.org/10.1016/j.rser.2017.05.278.

[14] Rossi I, Sorce A, Traverso A. Gas turbine combined cycle start-up and stress evaluation: A simplified dynamic approach. Appl Energy 2017;190:880–90. https://doi.org/10.1016/j.apenergy.2016.12.141.

[15] Kahlert S, Spliethoff H. Investigation of different operation strategies to provide balance energy with an industrial combined heat and power plant using dynamic simulation. J Eng Gas Turbines Power 2017;139:1–8. https://doi.org/10.1115/1.4034184.

[16] Angerer M, Kahlert S, Spliethoff H. Transient simulation and fatigue evaluation of fast gas turbine startups and shutdowns in a combined cycle plant with an innovative thermal buffer storage. Energy 2017;130:246–57. https://doi.org/10.1016/j.energy.2017.04.104.

[17] Sun S, Pasha A. HRSGs for Combined Cycle Plants: Design Considerations and Life Consumption Estimation Using Dynamic Software. In: Proceedings of the ASME 2011 Power Conference; 2011. p. 1–14.

[18] Yoshida Y, Yamanaka K, Yamashita A, Iyanaga N, Yoshida T. Coordinated Control of Gas and Steam Turbines for Efficient Fast Start-Up of Combined Cycle Power Plants. J Eng Gas Turbines Power 2017;139. doi:10.1115/1.4034313.

[19] Dooley B, Anderson B. Trends in HRSG Reliability – A 10-Year Review. Power Plant Chem 2019;21:158–88.

[20] Briola S, Gabbrielli R, Delgado A. Energy and economic performance assessment of the novel integration of an advanced configuration of liquid air energy storage plant with an existing large-scale natural gas combined cycle. Energy Convers Manag 2020;205:112434. https://doi.org/10.1016/j.enconman.2019.112434.

[21] Poblete IBS, Araujo O de QF, de Medeiros JL. Dynamic analysis of sustainable biogas-combined-cycle plant: Time-varying demand and bioenergy with carbon capture and storage. Renew Sustain Energy Rev 2020;131. doi:10.1016/j.rser.2020.109997.

[22] Li D, Hu Y, Li D, Wang J. Combined-cycle gas turbine power plant integration with cascaded latent heat thermal storage for fast dynamic responses. Energy Convers Manag 2019;183:1–13. https://doi.org/10.1016/j.enconman.2018.12.082.

[23] Angerer M, Djukow M, Riedl K, Gleis S, Spliethoff H. Simulation of Cogeneration-Combined Cycle Plant Flexibilization by Thermochemical Energy Storage. J Energy Resour Technol Trans ASME 2018;140. doi:10.1115/1.4038666.

[24] Bartnik R, Buryn Z, Hnydiuk-Stefan A. Thermodynamic and economic analysis of effect of heat accumulator volume on the specific cost of heat production in the gas-steam CHP plant. Energy 2021;230:120828. https://doi.org/10.1016/j.energy.2021.120828.

[25] Ortiz C, Chacartegui R, Valverde JM, Carro A, Tejada C, Valverde J. Increasing the solar share in combined cycles through thermochemical energy storage. Energy

Convers Manag 2021;229:113730. https://doi.org/10.1016/j.enconman.2020.113730.
[26] Gao Z, Ji W, Guo L, Fan X, Wang J. Thermo-economic analysis of the integrated bidirectional peak shaving system consisted by liquid air energy storage and combined cycle power plant. Energy Convers Manag 2021;234:113945. https://doi.org/10.1016/j.enconman.2021.113945.
[27] Rao AG, van den Oudenalder FSC, Klein SA. Natural gas displacement by wind curtailment utilization in combined-cycle power plants. Energy 2019;168:477–91. https://doi.org/10.1016/j.energy.2018.11.119.
[28] Zhao Y, Zhao CY, Markides CN, Wang H, Li W. Medium- and high-temperature latent and thermochemical heat storage using metals and metallic compounds as heat storage media: A technical review. Appl Energy 2020;280. doi:10.1016/j.apenergy.2020.115950.
[29] Mahdi JM, Mohammed HI, Talebizadehsardari P, Ghalambaz M, Sh. Majdi H, Khan A, et al. Simultaneous and consecutive charging and discharging of a PCM-based domestic air heater with metal foam. Appl Therm Eng 2021;197:117408. doi:10.1016/j.applthermaleng.2021.117408.
[30] Hajjar A, Mehryan SAM, Ghalambaz M. Time periodic natural convection heat transfer in a nano-encapsulated phase-change suspension. Int J Mech Sci 2020;166. doi:10.1016/j.ijmecsci.2019.105243.
[31] Stevanovic VD, Petrovic MM, Milivojevic S, Ilic M. Upgrade of the thermal power plant flexibility by the steam accumulator. Energy Convers Manag 2020;223:113271. https://doi.org/10.1016/j.enconman.2020.113271.
[32] Richter M, Oeljeklaus G, Görner K. Improving the load flexibility of coal-fired power plants by the integration of a thermal energy storage. Appl Energy 2019;236:607–21. https://doi.org/10.1016/j.apenergy.2018.11.099.
[33] Trojan M, Taler D, Dzierwa P, Taler J, Kaczmarski K, Wrona J. The use of pressure hot water storage tanks to improve the energy flexibility of the steam power unit. Energy 2019;173:926–36. https://doi.org/10.1016/j.energy.2019.02.059.
[34] Khare S, Dell'Amico M, Knight C, McGarry S. Selection of materials for high temperature sensible energy storage. Sol Energy Mater Sol Cells 2013;115:114–22. https://doi.org/10.1016/j.solmat.2013.03.009.
[35] EPRI. Electric Power Research Institue, Evaluation of Thermal-, Creep- and Corrosion-Fatigue of Heat Recovery Steam Generator Pressure Parts. EPRI, Palo Alto, CA. 1010440. vol. 3; 2006.
[36] Kumar N, Besuner P, Lefton S, Agan D, Hilleman D. Power Plant Cycling Costs. Report NREL/SR-5500-55433; 2012.
[37] Hoivik N, Greiner C, Barragan J, Iniesta AC, Skeie G, Bergan P, et al. Long-term performance results of concrete-based modular thermal energy storage system. J Energy Storage 2019;24:100735. https://doi.org/10.1016/j.est.2019.04.009.
[38] Salomoni VA, Majorana CE, Giannuzzi GM, Miliozzi A, Di Maggio R, Girardi F, et al. Thermal storage of sensible heat using concrete modules in solar power plants. Sol Energy 2014;103:303–15. https://doi.org/10.1016/j.solener.2014.02.022.
[39] Kindi AA Al, Pantaleo AM, Wang K, Markides CN, Kingdom U. Thermodynamic Assessment of Steam-Accumulation Thermal Energy. 11th Int Conf Appl Energy (ICAE 2019); 2019.
[40] Benato A, Bracco S, Stoppato A, Mirandola A. LTE: A procedure to predict power plants dynamic behaviour and components lifetime reduction during transient operation. Appl Energy 2016;162:880–91. https://doi.org/10.1016/j.apenergy.2015.10.162.
[41] Bergman TL, Lavine AS, Incropera FP, DeWitt DP. Fundamentals of heat and mass transfer. Seventh Edition. Jefferson City: United States. John Wiley & Sons; 2011.
[42] Tamme R, Laing D, Steinmann WD. Advanced thermal energy storage technology for parabolic trough. J Sol Energy Eng Trans ASME 2004;126:794–800. https://doi.org/10.1115/1.1687404.
[43] Bai F, Xu C. Performance analysis of a two-stage thermal energy storage system using concrete and steam accumulator. Appl Therm Eng 2011;31(14-15):2764–71. https://doi.org/10.1016/j.applthermaleng.2011.04.049.
[44] Serth RW, Lestina TG. Process Heat Transfer: Principles, applications and rules of thumb. Elseveir Inc., Second Edition. 2014. https://doi.org/10.1016/B978-0-12-397195-1.00005-4.
[45] Madani Sani F, Huizinga S, Esaklul KA, Nesic S. Review of the API RP 14E erosional velocity equation: Origin, applications, misuses, limitations and alternatives. Wear 2019;426–427:620–36. https://doi.org/10.1016/j.wear.2019.01.119.
[46] Prieto C, David P, Gonzalez-roubaud E, Fereres S, Cabeza LF. Advanced Concrete Steam Accumulation Tanks for Energy Storage for Solar Thermal Electricity. Energies 2021;14(3896):1–26. https://doi.org/10.3390/en14133896.
[47] Byrne RC. Standards of the tubular exchangers manufacturers association, 8th ed. Tubular Exchanger Manufactures Association (TEMA). New York, United States; 1999.
[48] Sakata M, Sasaki S, Mantovani P, Ngomo V. Application of SA-533 Class 2 Vessels in Floating LNG Plants. Paper No: PVP2020-21712, V006T06A054; 8 pages. ASME 2020 Press. Vessel. Pip. Conf., 2020. doi:10.1115/PVP2020-21712.
[49] Åström KJ, Bell RD. Drum-boiler dynamics. Automatica 2000;36(3):363–78. https://doi.org/10.1016/S0005-1098(99)00171-5.
[50] Stevanovic Vladimir D, Petrovic Milan M, Milivojevic Sanja, Maslovaric Blazenka. Prediction and control of steam accumulation. Heat Transf Eng 2015;36(5):498–510. https://doi.org/10.1080/01457632.2014.935226.
[51] Montes MJ, Abánades A, Martínez-Val JM, Valdés M. Solar multiple optimization for a solar-only thermal power plant, using oil as heat transfer fluid in the parabolic trough collectors. Sol Energy 2009;83(12):2165–76. https://doi.org/10.1016/j.solener.2009.08.010.
[52] ASME. American Society of Mechanical Engineers. ASME Boiler and pressure vessel code. Section II, Part D Properties, Materials; 2010.
[53] Seider W, Seader J, Lewin D, Widagdo S. Product and Process Design Principles, Synthesis, Analysis and Evaluation. Third Edition. John Wiley; 2009.
[54] Tycoon_Piping_Solutions. SA213 T22 Seamless Tube 2021. https://www.oilandgaspipingmaterials.com/astm-a213-sa213-t22-alloy-steel-tube-suppliers.html (accessed May 1, 2021).
[55] SendeCO2. European system of CO2 negotiation 2021. https://www.sendeco2.com (accessed September 8, 2021).
[56] Li W, Wei P, Zhou X. A cost-benefit analysis of power generation from commercial reinforced concrete solar chimney power plant. Energy Convers Manag 2014;79:104–13. https://doi.org/10.1016/j.enconman.2013.11.046.
[57] MITECO. Spanish Ministry for Ecological Transition and the Demographic Challenge. Register of carbon footprint, compensation and carbon dioxide absorption projects 2021 2021. https://www.miteco.gob.es/es/cambio-climatico/temas/mitigacion-politicas-y-medidas/factoresemision_tcm30-479095.pdf (accessed September 8, 2021).
[58] Sabugal S, Gómez F. Centrales Térmicas de Ciclo Combinado. Endesa: Teoría y Proyecto. Ediciones Diaz de Santos; 2006.
[59] CHANGBAO. HRSG super long boiler tubes 2021. http://en.cbsteeltube.com/product/HRSG-super-long-boiler-tubes.html.
[60] ZhongshunSteelPipe. Heat Recovery Steam Generators super long boiler tube 2021. https://www.zssteeltube.com/hrsg-boiler-tube/.